

**PROBABILISTIC SEISMIC HAZARD MAP
OF KYRGYZSTAN (CENTRAL ASIA):
APPLICATION TO THE REGIONAL HAZARD
OF SEISMICALLY INDUCED LANDSLIDES**

***H.-B. Havenith¹, Philippe Trefois², D. Jongmans¹,
K. Abdrakhmatov³, D. Delvaux²***

¹: Laboratory of Geophysics, University of Liege, Liege

²: Department of Geology, Royal Museum of Central Africa, Tervuren

³: Kyrgyz Institute of Seismology, Bishkek

Belgium, Kyrgyz Republic

Summary

In the frame of the project called 'Landslides triggered by earthquakes in Kyrgyzstan, Tien Shan' different probabilistic seismic hazard maps of Kyrgyzstan were built. While PGA maps are important for civil engineering structures, Arias intensity maps are used as input for hazard calculations of seismogenic landslides. On a GIS platform, the Arias intensity map as well as geotechnical, geological and morphological information were compiled to estimate the hazard of seismically induced landslides for the Suusamyr region, Kyrgyzstan. We applied the method of Jibson et al. (1998) using the concept of the Newmark displacement.

Seismic zones and their activity

The seismic catalogue of Kyrgyzstan contains data of more than 69000 earthquakes. The whole catalogue covers a period of about 2250 years, with historical data beginning in 250 BP and first instrumental records beginning in 1960. The data of this catalogue as well as geological and tectonic information were compiled to outline two types of seismic zones.

At first, Kyrgyzstan was divided in six large tectonic zones : northern Tien Shan, northeastern Tien Shan, central Tien Shan, southeastern Tien Shan - northern Tarim basin, southern Tien Shan - northern Pamir and finally the western Tien Shan (Figure 1).

Secondly, inside these large areas, zones of an increased historical and instrumental seismicity have been outlined (Figure 1). The extension of these smaller zones is directly depending on fault traces that have been studied on satellite images as well as on geological maps. In the northern Tien Shan area, mainly three zones present a higher seismicity : the southern Chu basin

НАЦИОНАЛЬНАЯ АКАДЕМИЯ НАУК
КЫРГЫЗСКОЙ РЕСПУБЛИКИ

ИНСТИТУТ ФИЗИКИ И
МЕХАНИКИ ГОРНЫХ ПОРОД

ПРОБЛЕМЫ
ГЕОМЕХАНИКИ
И
ГЕОТЕХНИЧЕСКОГО
ОСВОЕНИЯ
ГОРНЫХ ТЕРРИТОРИЙ

Труды международной конференции,
посвященной 40-летию ИФимГП НАН КР
и международному Году гор
(Бишкек, 4–6 октября 2000 г.)

Под общей редакцией
академика НАН КР,
профессора *И.Т. Айтматова*

Издательство «Илим»
Бишкек • 2001

including several historical events of a Magnitude higher than six; the Suusamyр basin with the recent $M_s=7.3$ Suusamyр earthquake in 1992 and the Kemin region affected in 1911 by the strongest historical earthquake in Kyrgyzstan, the Kemin earthquake of an estimated magnitude of 8.2. Inside the northeastern Tien Shan zone, only one zone has been defined on the base of a large historical earthquake in 1716 of a magnitude of 7.5. The central Tien Shan, delimited in the west by the Talas Fergana fault includes two seismic zones corresponding respectively to the Naryn and Issyk Kul regions, both characterised by a medium seismicity. Inside the area at the border between the Tien Shan and the Tarim basin, four zones present a very strong seismic activity : the Pik Pobedi region, the southern and northern Kepintage thrust fault zones and a zone North of Kashgar. Close to the southern Tien Shan border, a seismically active zone West of Kashgar and a zone along the seismically active Pamir thrust fault have been outlined. Inside the western Tien Shan area delimited in the East by the Talas Fergana fault four zones have been defined : the tectonically active rim around the Fergana basin, a small southwestern zone, a northwestern zone and a northern zone affected by the Tchatkal earthquake in 1946 of a magnitude of 7.4. Thus, besides the six large tectonic zones, 16 small seismically active zones were defined.

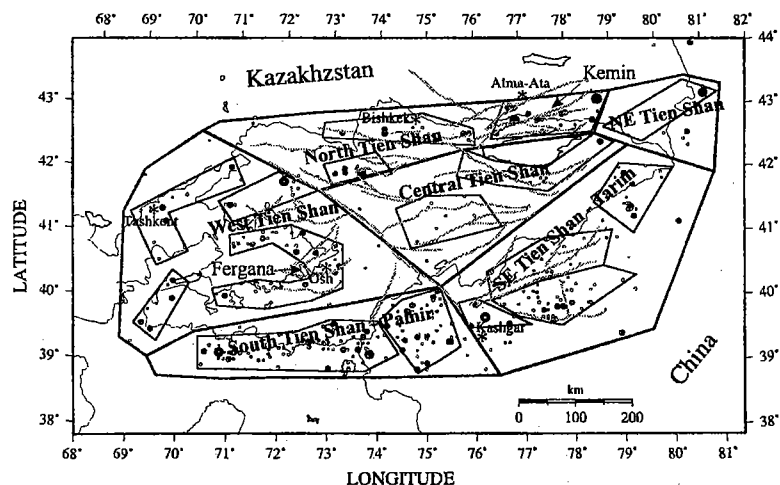


Figure 1 : Historical and instrumental earthquakes with a magnitude greater than 5 in Kyrgyzstan and bordering areas. Large dark grey circles are earthquakes with a magnitude greater than 7. Bolt contours delimit the six large tectonic zones, the thin contours delimit the sixteen small seismic zones.

Seismic hazard map of Kyrgyzstan

In order to quantify the seismicity of all these 22 zones, the Gutenberg-Richter law was calculated on the base of the seismic catalogue. Since we observed a strong contrast between the number of events per year before and after 1960, the installation of the first Kyrgyz seismic network, only instrumental data were considered for defining the Gutenberg-Richter law (equation 1):

$$\log(N/Yr) = a \cdot M + b \quad (\text{equation 1})$$

The two parameters 'a' and 'b' in equation 1, entirely permit to characterise the seismicity of a region. The 'a' parameter defines the global level of seismicity, while the slope 'b' parameter, theoretically between 0.7 and 1.3 expresses the weight of large earthquakes with respect to small ones : low 'b' values characterise a seismicity with a larger weight of strong earthquakes, high 'b' values indicate a larger weight of small earthquakes. The Gutenberg-Richter laws for the northern Tien Shan area is shown in figure 2a. Figures 2b and 2c show the law for two small zones, the rim around the Fergana basin and the Kemin zone. Compared with the region around the Fergana basin, the Kemin region is characterised by a lower 'b' values that indicates a higher occurrence probability for strong earthquakes.

The Gutenberg-Richter law for each zone is introduced in the input file for the SEISRISK3 program (Bender and Perkins, 1987), which calculates the seismic hazard in terms of Peak Ground Acceleration (PGA). The second information needed for seismic hazard estimates is the geometry of the seismic zones. Finally, the input file also includes a table describing the attenuation of acceleration over distance. In the case of Kyrgyzstan there were not enough strong data available neither to determine an attenuation law for the specific zones nor for the whole area of Kyrgyzstan. Therefore, different kinds of attenuation laws were applied to the seismic hazard map of Kyrgyzstan. The first law that was used is the smooth law introduced by Ambraseys (1996) for Europe. Another law applied is the one defined by Peng et al. (1985) for the northern Himalaya, a third law that was tested has also been applied by Zhang et al. (1999) to China and areas in the vicinity. All seismic hazard maps of Kyrgyzstan were calculated for 3 periods of 50, 100 and 250 years with probability of 90% of non-exceedance.

First, a general seismic map was calculated on the base of the six large tectonic zones and with the smooth law by Ambraseys (1996). The PGA values over Kyrgyzstan range between 0.4 g in the Southeast and 0.1 g in the Northwest. The second map (Figure 3) was calculated for same attenuation law, but all 16 small seismic zones were considered in addition to the 6 large zones. The effect of these small zones on the seismic hazard a stronger lateral variation of PGA between maximum and minimum values of 0.55 g and 0.1 g.

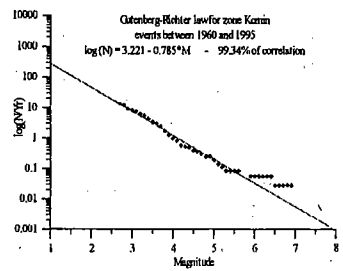
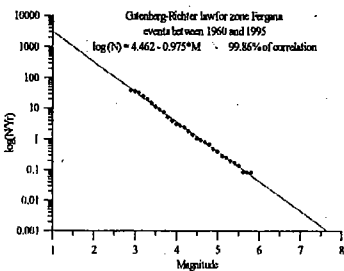
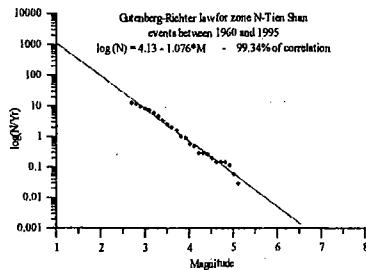


Figure 2 : Gutenberg-Richter laws for the northern Tien Shan region (a), the rim around the Fergana basin (b) and the Kemir region (c) (see Figure 1 for location).

An even stronger variation PGA values between 0.85 g and 0.1g is obtained if the law of Peng et al. (1985). The law of Zhang (1999) gives analogue results

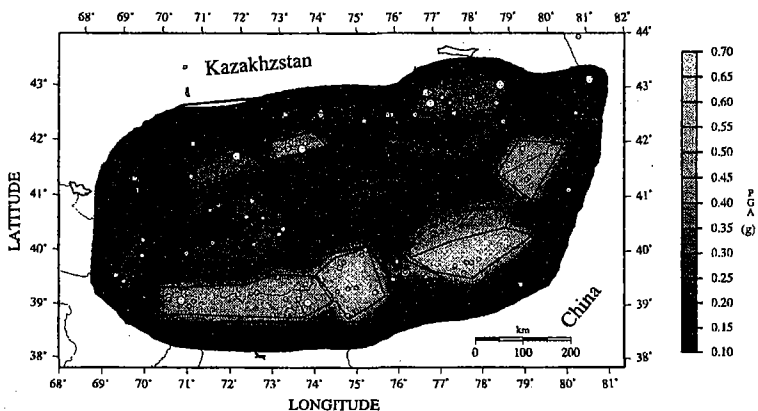


Figure 3 : Seismic hazard map using an attenuation law obtained by stochastic simulation of earthquakes.

We have also tried to define a new attenuation law for Kyrgyzstan by simulating strong motion records for different magnitudes and distances. These simulations done with the program developed by Boore (1996) were constrained by the different existing attenuation laws and by the few actual PGA data. The resulting map for this simulated law is shown in Figure 3. Since this map was based on different laws and on the data themselves, we think that it presents the best estimates of seismic hazard over Kyrgyzstan. If we compare this map with the two actually existing seismic hazard maps of China and the Russian federation including also Kyrgyzstan presented respectively by Zhang et al. (1999) and by Ulomov et al., 1999), it appears that mean PGA values of our map are slightly lower. But maximum PGA values compare well with the existing maps.

The Arias intensity map

Besides its application to PGA hazard maps, the procedure applying simulated earthquakes permits also to calculate the Arias intensity, I_a (equation 2), and to define an attenuation law for this latter.

$$I_a = \frac{\pi}{2g} \int_0^t a^2 dt \quad \text{equation 2}$$

- I_a : Arias intensity (m/s)
- a : ground acceleration (m/s²)
- t : duration of the strong motion recording (s)
- g : 9.81 m/s²

We calculated an probabilistic Arias intensity map of the whole area of Kyrgyzstan, but here only a part is shown, the Arias intensities over the Suusamyр region (Figure 4). In fact, this part was used to calculate the hazard of seismogenic landslides following the method of Jibson et al. (1998). First, a map of static Factors of safety (FS) is calculated on the base of a slope map, a geotechnical map with c , ϕ values, and a surface layer thickness map. The slope map is obtained from a digitised topographical map of the region. The geotechnical map is simply based on the geological map (Figure 5), where c , ϕ and volumic weight values have been attributed to the geological formations (table 1).

The values presented in table 1 were obtained from references (Hoek and Bray, 1981; Philipponnat, 1979) or have been directly measured on samples taken from trenches in the Suusamyр valley (see Havenith et al., this conference).

Table 1

Geotechnical parameters for the geological units shown in Figure 5.

Rock	Cohesion C (MPa)	Friction angle ϕ (°)	volumic weight γ (kg/m ³)
Quaternary, alluvial, glacial	0.02	26	2.05
Neogene, silt and claystone	0.07	24	2.45
Granite	0.05	34	2.55
Paleozoic sediments	0.1	32	2.45
Paleozoic volcanics	0.05	27	2.75

For the whole map, the thickness of the layer prone to sliding has been fixed at 10m, because we think that the method is better adapted to denudation prediction than to prediction of deep seated landslides. The saturation of the layer has been estimated at 50% (5 m out of the 10 m). Combining all the mentioned parameters, it is possible to calculate a certain FS (equation 3) per pixel of the map, which contains 1160*440 pixels (Figure 6).

$$FS = \frac{c}{g \cdot t \cdot \sin \alpha} + \frac{\tan \phi}{\tan \alpha} - \frac{m \cdot \gamma_w \cdot \tan \phi}{\gamma \cdot t \cdot \tan \alpha} \quad \text{equation 3}$$

FS : Factor of safety

c : cohesion (MPa)

ϕ : phi (°)

α : slope angle (°)

t : total layer thickness (m)

m : thickness of saturated layer

γ : volumic weight – dry (kg/m³)

γ_w : volumic weight – wet (kg/m³)

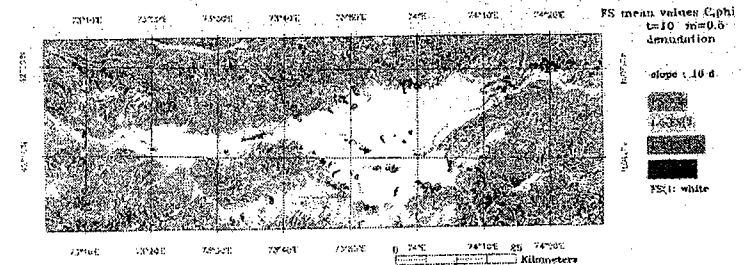


Figure 6 : Map (1160*440 pixel) of the Suisamy region presenting one FS values per pixel.

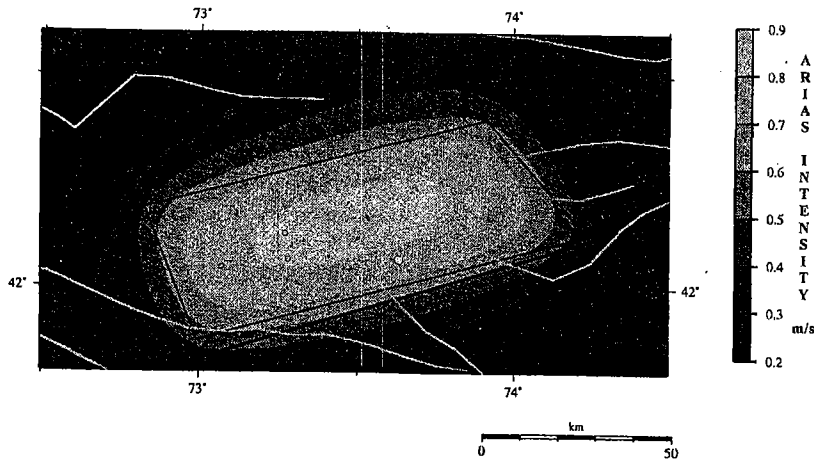


Figure 4 : Arias Intensity map over the Suisamy region. The white circle marks the epicentre of the Ms=7.3 Suisamy earthquake in 1992.



- Quaternary
- ▨ Neogene
- ▩ Paleozoic granite
- ▧ Paleozoic volcanics
- Paleozoic sediments

Figure 5 : Simplified geological map of the Suisamy region, with five distinguished geological units.

For slope angles lower than 10°, no FS were calculated, because the resulting FS becomes very high and can not be included in the following pseudo-static approach.

Pseudo-static conditions: Newmark displacement

Newmark's method (Newmark, 1965) is based on a simple model of a block sliding on a plane. It is calculated on the base of the critical acceleration, i.e. the threshold acceleration required to initiate sliding. As can be seen from equation 4, the critical acceleration depends on the FS and on the slope angle.

$$a_c = (FS - 1) \cdot g \cdot \sin \alpha \quad \text{equation 4}$$

- a_c : critical acceleration (m/s²)
- FS : Factor of safety
- g : 9.81m/s²
- α : slope angle (°)

This formula was neither computed for $\alpha < 10^\circ$ as mentioned above nor for an FS < 1.

Different formulas link the Newmark displacement to arias intensity and to the critical acceleration. We have chosen the one introduced by Miles and Ho (1999) given in equation 5: The map of final displacements is shown in figure 7.

$$\log(D) = 1.46 \cdot \log(Ia) - 6.642 \cdot a_c + 1.546 \quad \text{equation 5}$$

- D : Newmark displacement (cm)
- Ia : Arias intensity (m/s)
- a_c : critical acceleration (m/s²)

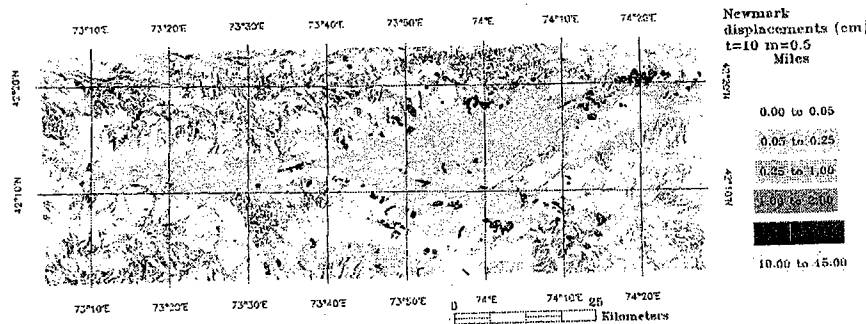


Figure 7 : Map of Newmark displacements with actual landslides plotted.

Final displacements are quite small compared with the large landslides plotted on the map. First, this is due to the fact that Newmark displacement does not take into account aseismic (some landslides plotted are aseismic) or post-seismic displacements. Other reasons are that many processes have been strongly simplified, such as dynamical aspects or hydrological conditions.

As conclusion, we may say that larger Newmark displacements hint at risk zones but do actually not predict real displacements. A further step is to calculate the probability of landslide occurrence with respect to the calculated displacements as proposed by Jibson et al. 1998, this work has not yet been completed.

References

1. N.N. Ambraseys, K.A. Simpson and J.J. Bommer (1996). Prediction of horizontal response spectra in Europe. EESD, 25, 371-400.
2. B. Bender and D.M. Perkins (1987). SEISRISKIII: A computer program for seismic hazard estimation. USGS, 1772.
3. Boore, D.M. (1996). 'SMSIM-Fortran programs for simulating ground motions from earthquakes : version 1.0'. U.S. Geol.Surv., Open-File Rept.96-80-A, pp.73.
4. Hoek, E. and Bray, J. (1981). 'Rock slope engineering'. Institution of Mining and metallurgy. pp.358.
5. R.W. Jibson, E.L. Harp and J.A. Michael (1998). A method for producing digital probabilistic seismic landslide hazard maps: an example from the Los Angeles, California, Area. Open-File Report 98-113.
6. Miles, S.B. and Ho, C.L. (1999). Rigorous landslide hazard zoning using Newmark's method and stochastic ground motion simulation. Soil Dyn. and Earthquake Engin., 18, 305-323.
7. Newmark, N. : (1965). Effects of earthquakes on dams and embankments', Géotechnique, 15, 2, 137-160.
8. K.-Z. Peng, F.T. Wu and L. Song (1985). Attenuation characteristics of peak horizontal acceleration in Northeast and Southwest China. EESD, 13, 337-350.
9. Philipponnat G. (1979). Fondations et ouvrages en terre'. Ed. Eyrolles, pp. 402.
10. V.I. Ulomov and the GSHAP Region 7 working group (1999). Seismic hazard of Northern Eurasia. Annali di Geofisica, 42,6, 1023-1038.
11. P. Zhang, Z. Yang, H.K. Gupta, S.C. Bhatia and K.M. Shedlock (1999). Global seismic hazard assessment program (GSHAP) in continental Asia. Annali di Geofisica, 42, 6, 1167-1190.